



A Comprehensive Study on the Effects of Contamination, Hydrophobicity and Dry-bands on the Leakage Current of Silicone Rubber Insulators

Mohammad Mahdi Manzari Tavakoli¹ and Seyed Mohammad Hassan Hosseini^{1,*}

ARTICLE INFO

Article history:

Received: 21 February 2021

Revised: 7 August 2021

Accepted: 29 August 2021

Keywords:

Silicon rubber insulators

FEM

Leakage current

Hydrophobicity

ABSTRACT

The present study was carried out in order to investigate the effects of hydrophobicity and dry-band arcing on leakage current in both time and frequency domains. The impacts of these phenomena on electric and potential field distributions are observed and analysed. Also, this paper studies the measurement methods for pollution accumulated on insulator surface. From the results, it is concluded that the third and seventh harmonics, the third to fifth harmonics ratio and the amplitude of leakage current are increased in the polluted insulator surface compared to the condition in which the insulator surface is clean and hydrophobic. Therefore, the dry-band arcing occurs. Besides, it can be observed that the growth rate of the third harmonic is higher than the fundamental harmonic, indicating the critical condition of the insulator with more clarity. In the proposed method, the analysis of the insulator behavior can be performed with greater accuracy as opposed to traditional methods analyzing the insulator behavior just by monitoring the peak value and the fundamental harmonic. The severity of contamination is measured through calculating the equivalent salt deposit density and non-soluble deposit density. The simulation results by Finite Element Method (FEM) confirm that the electric field is directly proportional to the probability of the surface arcing.

1. INTRODUCTION

The surface hydrophobicity of the high voltage insulators such as Silicone Rubber (SiR) insulators has been of great interest in recent years as a demanded feature in distribution systems [1]. Deposition of contaminant on the insulators has turned into a challenging issue in transmission systems due to the fact that surface flashover can either reduce the reliability or lead to failure of the system [2]. A combination of contaminants and humidity can create the conductive areas and leakage current [3]. The leakage current density is not uniform across the insulator surface. thus, the temperature in some areas of the insulator surface may rise, leads to the creation of dry-bands. Therefore, the voltage redistribution on the hydrophilic surfaces because of aging and deposits of contamination causes high electric fields across these dry-bands. As a result, partial arcs may happen. Insulating material in polymeric insulators would be eroded and chemically degraded due to partial arcs. Expansion of the partial arc in conditions of low surface resistance eventually causes the flashover of the insulator [4]. Two different types of discharges, which can indicate the insulation performance, are generally observed in high voltage insulators. One is corona partial discharge

occurring between water drops on a wet surface, and the other is dry-band arc discharge between dry bands on a polymeric material surface. The destruction severity of dry band arc discharge is more than that of corona discharge. This may cause aging and hydrophilic phenomenon due to erosion in insulator material [5]. Consequently, the measurement of contamination and monitoring the insulator surface condition can hold a significant impact on the power quality and reliability of the power system. Offline and online techniques can be employed for analysis of the insulator surface in terms of contamination measurement. A general method to access the severity of contamination, presented by IEC 60815, is cleansing the insulator surface by a specific volume of water and estimating the equivalent salt deposit density (ESDD) and non-soluble deposit density (NSDD) directly. The severity of contamination can be specified with regard to ESDD which causes electrical conduction and NSDD which contributes to water retention. However, continuous measurement of the leakage current or the electric field in polluted areas by online monitoring is mostly preferred over the limitedly applicable offline methods [6]. The information concerning the severity of contamination, flashover and the insulator surface condition can be

¹Department of Electrical Engineering, South Tehran Branch, Islamic Azad University, Tehran, Iran.

*Corresponding author: Seyed Mohammad Hassan Hosseini; Email: smhh110@azad.ac.ir.

provided by online monitoring of the leakage current through the surface of the insulator. The conducted studies on the measurement of leakage current can be classified into four groups [7]:

- Applications of time-domain approaches to electrical values, including peak value, phase shift, and accumulated charge [4, 7, 8].

- Applications of frequency-domain approaches such as harmonic detection algorithms using Fast Fourier Transform (FFT) analysis and wavelet method [3].

- Pattern-recognition methods such as statistical pattern recognition, recurrent analysis and artificial neural networks (ANN) [9, 10].

- Standard deviation multi-resolution analysis (STD-MRA) method used for pattern analysis and frequency analysis [4, 9, 11].

In [1], the severity of contamination is determined by measurement of the pulse number, the leakage current peak and the values of cumulative charge. The insulator condition can also be evaluated by calculation of the phase difference between the leakage current and the applied voltage together with the maximum pulse amplitude via a method proposed by [12]. Regarding the occasional incompatibility of the peak value with the arcing activity in the peak detection method, the third and fifth harmonic along with the fundamental component were incorporated in a diagnostic tool as an alternative method in order to assess the performance of silicone rubber insulator in salt fog environments [13]. In [4], discrete wavelet transform (DWT) decomposition has been used and standard deviation multi-resolution analysis (STD-MRA) distortion ratio pattern of the leakage current has been adopted to evaluate the insulator surface pollution. Despite the fact that many studies have tried to predict and resolve the flashover phenomenon on the insulator surface by analyzing the leakage current, it can be found that only a few investigations have used the combined analysis in both time and frequency domains [14-15]. This paper presents an analytical study in time and frequency space to establish an accurate prediction in order to avoid flashover phenomenon and its undesirable implications. Herein, for provision of a better understanding of the insulator behavior, the electric field and potential distributions of hydrophilic and hydrophobic insulators in the presence of dry bands in both conditions of exposure and non-exposure to pollution were simulated.

2. EXPERIMENTAL IMPLEMENTATION

In order to simulate the clean and salt fogs conditions, all tests have been performed in artificial climatic situations in a cube stainless steel chamber with dimensions of 2×2×2 meters with two nozzles. All data were recorded with a two-channel digital oscilloscope with sample rate of 156 kilo samples per second (KSPS). The experimental setup is

constituted of various components including capacitor divider for measurement, a shunt resistor, a high voltage variable-ratio transformer (20 kVA, 380 V / 0-100 kV, 50 Hz), control and data acquisition systems (DAQ), a digital oscilloscope and protection system which are shown in Figure.1. In the low voltage side, a variable-ratio transformer is placed before protection circuit to change the voltage applied to the sample.

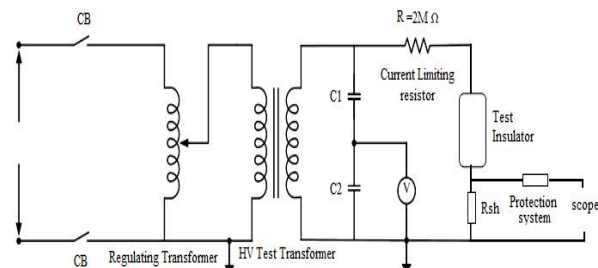


Fig. 1. Schematic of the fog chamber system.

2.1 Insulator profile

The experiments are conducted on a 20 kV Silicon Rubber insulator with characteristics presented in Table 1. Figure 2 demonstrates the tested insulator and relevant degree of hydrophobicity.

Table 1. Insulator Characteristics

Voltage class (kV)	Cree page distance (mm)	Shed diameters (mm)	Arcing distance (mm)	Mechanical tension strength (kN)
24	590	53-70	285	70

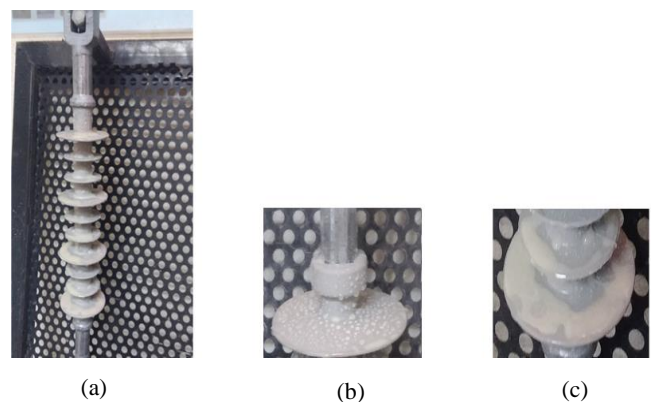


Fig. 2. (a) The tested insulator (b) the hydrophobicity degree of clean insulator surface, (c) The hydrophobicity degree of insulator surface after applying polluted layer.

2.2 Test procedure

The testing process consists of several steps. Initially, the insulator is washed to remove any kinds of impurities and grease. Afterwards, the cleansed insulator is exposed to

clean fog (without salt) vertically. After the insulator surface gets entirely wet, an 11.5 KV root-mean-square (RMS) voltage is applied. The next step is started with contamination the insulator surface. According to the solid layer method introduced by IEC 60507 standard, a mixture of Kaolin (40 g), salt (2 g) and water (1000 g) is considered. After drying and deposition of the above mentioned materials on the surface, both clean fog and salt fog with different salt concentrations are used to test the insulator. By appliance of an 11.5 KV RMS voltage to the insulator, the dry bands are formed due to the heat generated by the leakage current. Therefore, the dry-band arcing occurs because of the surface hydrophilicity. The leakage current in each modes was measured and recorded. Since the dry band arcing is one of the most critical and destructive states of the insulator operations, the leakage current in this condition was measured and analysed under different contamination severities.

In order to improve the analysis, the insulator behaviour was evaluated under stress conditions, and the leakage current's frequency characteristics were retrieved. The FFT was then used to transform the time-domain signal to the frequency domain and analyse these characteristics. By Equation (1), a time-domain signal ($F(t)$) can be converted into frequency domain ($F(f)$):

$$F(f) = \int_{-\infty}^{\infty} f(t)e^{-j2\pi ft} dt \quad (1)$$

The numerical integration was employed to compute the FFT providing approximate computations, namely discrete Fourier transform (DFT), as follows:

$$F_k = \sum_{n=0}^{N-1} f_n e^{-j2\pi kn/N}, k = 1, 2, \dots, N \quad (2)$$

Finally, the values of NSDD and ESDD of the insulator surface were measured.

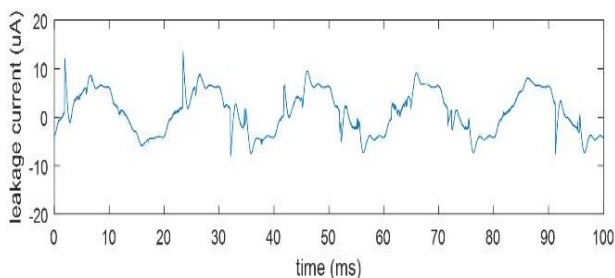


Fig. 3. Leakage current of the clean insulator in clean fog mode.

2.3. Leakage current of the clean insulator in clean fog mode

In this mode, the clean insulator was surrounded by clean fog, and no discharge could be observed. The leakage current and its third and seventh harmonic contents have short amplitudes. The fifth harmonic order is larger than third one, and the leakage current is sinusoidal. However,

there was a little distortion due to the environmental noise. The leakage current in this state is shown in Figure 3. Based on Figure 2(b), the degree of the surface hydrophobicity was placed in HC1 [16].

2.4. Leakage current of the polluted insulator

Due to the difficulty of polluting the surface of SiR Insulator associated with the hydrophobic nature of the material, the insulator surface has to be pre-polluted by the solid layer method based on IEC60507 standard in order to be able to uniformly spread the pollution and reduce the surface hydrophobicity [17]. In this mode, the primary coverage of the insulator surface with solid layer material results in a dramatic decrement in the surface hydrophobicity and the surface becomes hydrophilic (about HC4-HC6) as presented in Figure 2(c). Simultaneous presence of humidity and contamination on the insulator surface increases the leakage current in comparison with the other mode in which both the insulator and fog were clean. The asymmetrical leakage current distribution and non-homogeneous density throughout the surface of the insulator results in dry band formation. The major portion of the applied voltage was concentrated across the dry bands, causing the dry band arcing in the mentioned areas. Continuous dry band discharges may lead to degradation of the polymer material, CH and SiCH₃ bonds and erosion. Followed by destruction of the polymer lattice, the existing silicon on the surface of the insulator is decreased and the aluminum trihydrate (ATH) particles appear on the surface [5]. In sub-sections 2.4.1 to 2.4.2, the impacts of contamination degree on the leakage current were investigated by analysis of the pre-polluted insulator after dry band arcing in three modes including the clean fog, 15 g salt fog and 30 g salt fog.

2.4.1. Polluted insulator in clean fog condition

In this mode, the pre-polluted insulator was exposed to clean fog. After formation of dry-bands, the local arcs occur due to the surface hydrophilicity. It causes distortion in the leakage current and growth in magnitude of the third and seventh harmonic orders. The ratio of the third to fifth harmonic order is greater compared to the case of clean insulator. Figure 4(a) shows the leakage current waveform. In addition, the leakage current increases in response to the higher surface conductivity caused by the initial pre-pollution.

2.4.2. Polluted insulator in salt fog condition

This section investigates the effect of salt concentration in the applied fog on the leakage current.

2.4.2.1. Polluted insulator in salt fog with 15 g/L density

In this condition, the hydrophilic behavior of the surface leads to dry-band arcing due to implementation of the solid layer method and formation of dry-band areas. However, as the density of salt in fog is boosted to 15 g/L, the

conduction of the insulator surface is enhanced considerably resulting in addition of the amplitudes of the leakage current, the fundamental, third and seventh harmonic components, the ratio of the third to fifth harmonic orders and the number of arcing compared to the clean insulator condition. The leakage current in this mode is presented in Figure 4(b).

2.4.2.2. Polluted insulator in salt fog with 30 g/L density

Followed by increment of the density of salt in the fog to 30 g/L, the conduction of the insulator surface witnesses a notable rise. Based on Equation (3), this leads to a sharp increment in the amplitude of the leakage current. Figure 4(c) illustrates the leakage current waveform in this mode.

$$J = \sigma E \quad (3)$$

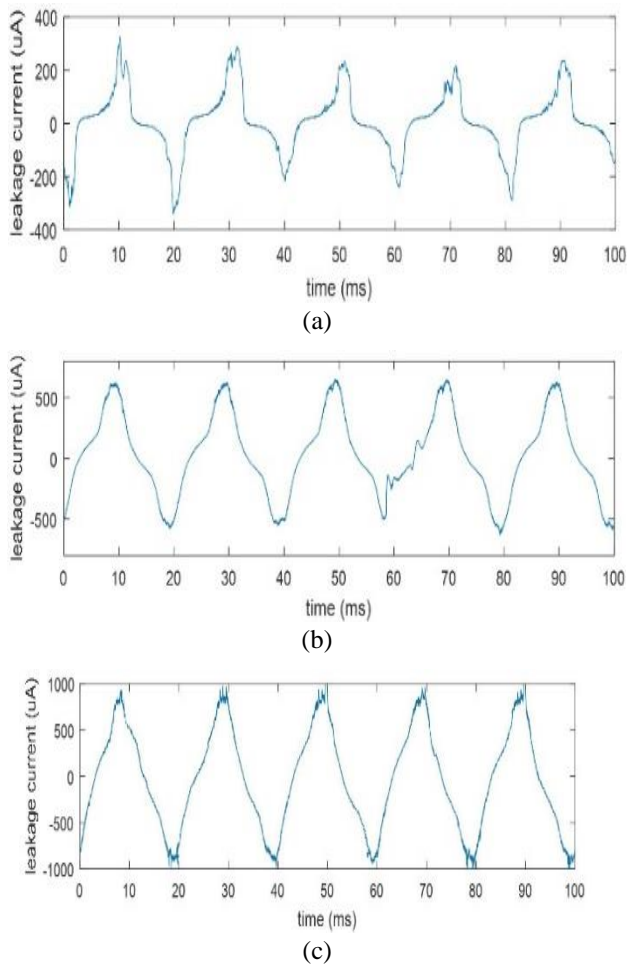


Fig. 4. Leakage current waveform polluted surface insulator in; (a) clean fog, (b) salt fog with 15 g/l density, (c) salt fog with 30 g/l density.

The hydrophilic behavior of the insulator surface can lead to occurrence of a great deal of arcing in the dry band areas which is potentially capable of turning into an overall flashover. If the applied power from the source becomes higher than the arcing power losses, and the overall wetting

rate of the insulator surface becomes more than its drying rate, a conductive path may be established on the surface, and the applied voltage can be placed across the dry bands. Thus, it is expected that the overall flashover will occur, and the local arcing of dry-bands will spread across the two electrodes of the insulator. In this case, the third harmonic constitutes a major proportion of all harmonic components, and the ratio of the third to the fifth and the magnitudes of the third and the seventh harmonics have a direct relationship with the surface condition and dry-bands arcing. Thus, the current waveform stay sinusoidal and the arcing do not occur as long as the third harmonic has smaller amplitude than fifth harmonic order. After showing the hydrophilic property by the insulator surface due to dry-bands, the partial arcing happens. As a consequence, the leakage current becomes distorted and non-sinusoidal. The third and seventh harmonic orders grow strongly, and the ratio of the third to fifth harmonic orders is far greater than the relevant ratio in the clean insulator condition. In comparison with the clean mode, it is also seen that the growth rate of the third harmonic was higher than the growth rate of the peak amplitude and the fundamental component. Thus, it can demonstrate the status of the insulator surface more effectively. Generally, the relationship between the severity of contamination deposited on the insulator surface and the leakage current can be summarized as following:

According to Equation (3), a rise in the conductivity of the insulator surface caused by the accumulated contamination can lead to increment of the leakage current amplitude. Therefore, the increase in the leakage current is directly proportional to the severity of the contamination, and is an indication of severity of contamination on the insulator surface. Furthermore, the accumulation of contamination on the hydrophobic surface results in temporary hydrophilicity of the surface, causing dry band arcing. As a consequence, the growth of the third and seventh harmonics and the ratio of the third to fifth harmonics compared to the normal operation in the clean and hydrophobic insulator surface can demonstrate an excessive contamination accumulated on the surface implying that the insulator surface needs to be washed, or in some cases, it should be replaced due to aging and erosion. Generally, the conduction of the insulator surface and the amplitudes of the third and seventh harmonic components are directly proportional to the probability of arcing on the surface. Meanwhile, the time and frequency analyses methods for investigating of deposited contamination density and the insulator surface condition is reliable and effective only when the surface is wet. All results are presented in Table 2.

Table 2. Harmonic components of insulator leakage current

STATE	Clean insulator clean fog	Pre polluted insulator clean fog	Pre polluted 15g/lit salty fog	Pre polluted 30g/lit salty fog
h_1	4	99	310	540
h_2	0.2	14	7	33.2
h_3	0.4	57	80	120
h_4	0.1	8	4	24.9
h_5	0.8	28	10	20
h_6	0.1	4	2	16.6
h_7	0.4	12	6	24.9
h_8	0.1	2	1	8.3
h_9	0.5	6	2	16.6
h_{10}	0.2	2	1	4.15
h_{11}	0.3	6	2	4.15
h_{12}	0.3	2	1	4.15
$\frac{h_3}{h_5}$	0.5	2.04	8	6
$\frac{h_3}{h_7}$	1	4.75	13.3	4.82
$\frac{h_{3(salt-fog)}}{h_{3(clean-fog)}}$	-	142.5	200	300
$\frac{h_{1(salt-fog)}}{h_{1(clean-fog)}}$	-	24.75	77.5	135
$\frac{A_{LC(salt-fog)}}{A_{LC(clean-fog)}}$	-	29.09	54.54	86.36

A_{LC} : the leakage current amplitude

3. EVALUATION OF CONTAMINATION

The distributed contamination on insulator surfaces may be categorized into two classes including soluble conductive pollution and insoluble nonconductive pollution. Equivalent salt deposit density (ESDD) and non-soluble deposit density (NSDD) can be used to calculate the density of soluble conductive and insoluble nonconductive pollutions on the SiR insulator surface. [2,18,19]. The quantity of surface pollutants is necessitated to be measured in the laboratory. The level of contamination is specified by measuring ESDD and NSDD according to IEC60815 standard. For the purpose of effective contamination measurement, the salt and water drops are wiped before drying the insulator. Next, the collected salt is dissolved in 500 mg distilled water, and the solution is stirred for more than two minutes. After that, the conductivity (S/m) and the temperature (°C) of the volume are measured. The volume conductivity at a temperature of 20 °C can be derived from Equation (4).

$$\sigma_{20} = \sigma_{\theta}(1 - b(\theta - 20)) \tag{4}$$

where, σ_{θ} denotes the conductivity of the volume at a temperature of $\theta(^{\circ}C)$ while b is the temperature dependent factor.

Equations (5) and (6) can be used to calculate the solution salinity (S_a) and the value of ESDD, respectively.

$$S_a = (5.7\sigma_{20})^{1.03} \tag{5}$$

$$ESDD = \frac{S_a \times V}{A} \tag{6}$$

where, A is the cleaned surface area (cm^2) and V is the solution volume (cm^3). For calculating NSDD by Equation (7), the filters are weighed before and after passage of the mentioned solution.

$$NSDD = 1000(w_f - w_i)/A \tag{7}$$

where, w_f the weight of filter is after passing contaminated solution and drying and w_i is the initial weight of the filter. Finally, according to IEC60815 standard, the severity of contamination is calculated considering ESDD and NSDD. The results are presented in Table 3.

4. SIMULATION RESULTS

The simulation of the electric field and potential distributions on the tested insulator at voltage ($20 \frac{\sqrt{2}}{\sqrt{3}}$) V applied to the lower electrode, and at 0 V applied to the upper electrode are performed and analyzed in Maxwell environment based on FEM method. The technical and environmental specifications of the simulated insulator are presented in Tables 4, 5.

Table 3. The severity of contamination of surface insulator

STATE	σ_{20}	S_a	ESDD	NSDD	Severity of contamination based on IEC60815
Pre polluted insulator clean fog	0.4	0.22	0.083	0.06	Medium and heavy borders
Pre polluted 15g/lit salty fog	1.1	0.62	0.238	0.11	Heavy
Pre polluted 30g/lit salty fog	2.5	1.44	0.553	0.14	Very heavy

Table 4. The assumed permittivity and conduction

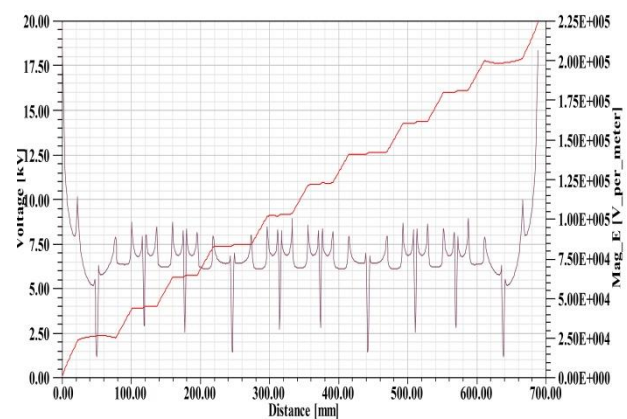
Material	Water droplets	Pollution layer	Pollution is mixed with film water	FRP	SiR	Air
Permittivity	83	15	20	7	3.45	1
Conductivity (S/m)	0.01	0	0.01	0	0	0

Table 5. The simulation parameters considered for insulator

Creepage distance	Sheds diameters	Dry bands length	Thickness of the hydrophilic surface water mixed to pollution film	Thickness of the pollution layer
680 mm	65-84 mm	20 mm	1 mm	1 mm

The results demonstrate that the electric field distribution is directly proportional to the discharge activity through composite insulators. The high electric field strength due to arcing caused by dry-bands and corona discharge can lead to erosion, aging and hydrophilic phenomenon in SiR insulator. Finally, it can extend an overall flashover through the insulator. Therefore, the intensity and distribution of the electric field of SiR Insulators needs to be taken into account. Hereon the simulation results concerning both clean and polluted modes are presented and assessed. The impacts of contamination, dry-band and hydrophobicity level on the electric field and potential distributions of SiR Insulator are investigated by analysis of the observation outcomes. In hydrophobic state, a new insulator was simulated before getting polluted (HC1), and in hydrophilic state, the simulation was carried out after applying solid layer pre-pollution, salt fog and insulator surface aging (HC6). The electric field and potential in the clean and dry insulator is illustrated in Figure 5(a) while the corresponding values to the polluted hydrophobic insulator and polluted hydrophilic insulator are illustrated in Figures 5(b)-(d) and Figure 6, respectively. The electric field intensity and the potential distribution are indicated by the purple and red lines respectively. According to the simulation results, the electric and potential intensity experienced less oscillations and values in the clean and dry surface insulator state. However, these parameters for the polluted hydrophobic state have shown more non-uniform distributions and higher values. Despite this issue, the insulator can still maintain its normal operation. In the polluted hydrophilic state, although the changes of the electric and potential intensity are negligible, their values are witnessed a dramatic rise after dry band forming. Therewith, the possibility of partial discharge increases significantly. In cases where the applied voltage is entirely high, the total flashover may happen because the partial discharge can extend through the insulator surface. In

accordance with Figure 5(c), the intensity of the applied electric field across dry-band area has a small value because of the hydrophobicity of the insulator surface, so it cannot cause a considerable dry-band arcing. However, based on Figure 5(d), when the wetting rate of insulator in the hydrophilic surfaces is more than its drying rate, the dry bands will not formed. Besides, the intensity of electric field will not have an extreme value, and insulator will operate in normal condition. On the other hand, when the drying rate of the hydrophilic insulator surface is more than wetting rate, the dry-bands are created due to asymmetric distribution of the leakage current. By applying artificial pollution and increasing the salt density in the applied fog, the conduction of insulator surface will rise. The higher surface conduction leads to decrease in the surface resistance. Furthermore; a large proportion of the applied voltage is concentrated across the dry-bands whereby the electric field is increased in the dry bands. This high electric field causes an extreme dry-band arcing and a significant growth in the third harmonic component. In another condition in which the rate of drying is much higher than the rate of wetting, the insulator surface dries so that the conductive path of the applied voltage to the dry-bands will disappear. Thus, the dry band arcing will be terminated. These results can contribute to a deeper comprehension of the insulator operation in presence of the dry-bands in contamination and humidity conditions. Combination of the obtained results with experimental observations of the leakage current, leads to a comprehensive analysis of the performance and behavior of the insulators in different states can be provided. It is noteworthy that the survey of the leakage current in terms of time-domain amplitude and harmonic levels along with the electric field distribution is a high performance method for analysis of the insulator surface statuses.



(a)

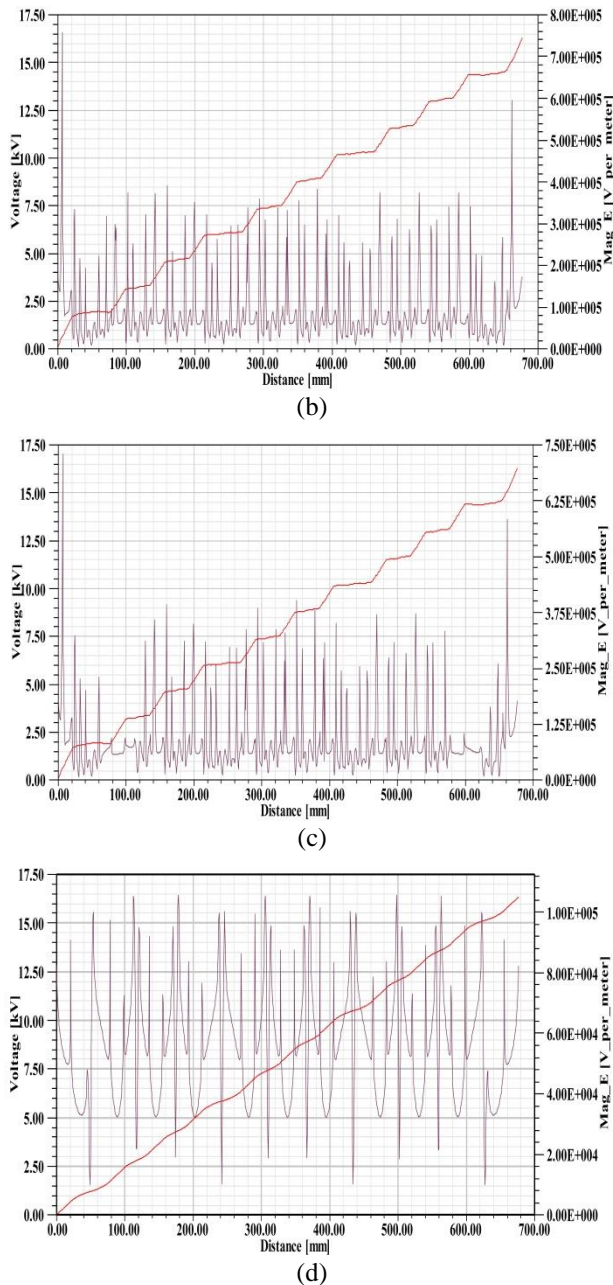


Fig. 5. The electric field and potential distributions across creepage distance; (a) the clean and dry insulator, (b) the polluted and hydrophobic insulator, (c) the polluted and hydrophobic insulator with upper and lower dry bands, (d) the polluted and hydrophilic insulator without dry bands.

5. CONCLUSION

The impacts of contamination severity, hydrophobicity, and dry-band areas on dry-band arcing and leakage current were studied analytically and comprehensively in this paper. This was followed by simulation and experimental validation of a sample insulator in

laboratory environment. On the surface of insulator, simulations of the electric field and potential distributions were performed, and the analyses were carried out in both time and frequency domains. Based on results, when the insulator surface was clean and hydrophobic, the amplitude of the fifth harmonic was higher than third harmonic, and the third and seventh harmonics had small amplitudes. There was no arcing in this mode and the leakage current waveform was sinusoidal. However, for the other mode with hydrophilic contaminated surface, the dry-band areas were formed and the third and seventh harmonics experienced a sharp increment individually. In such condition, the third harmonic became larger than fifth harmonic, the dry-band arcing occurred in dry areas, and a serious distortion was observed in the leakage current. Besides, it was confirmed that with increasing the severity of contamination on the surface of insulator, the intensity of dry-band arcing and amplitude of the leakage current and the third harmonic significantly expanded. The third harmonic growth rate compared to the fundamental component and the current peak was considerably higher. Therefore, the analysis of the insulator surface condition can be performed with more accuracy. A close relationship between electric field intensity, the dry-band arcing, and the leakage current were observed by analysing the simulation results. Accordingly, coexistence of humidity and pollution did not significantly affect the insulator operation as far as the insulator surface was hydrophobic. Nevertheless, once the surface became hydrophilic due to aging or coating, the combination of humidity, pollution and dry-bands led to an intense electric field across the dry-bands and occurrence of dry-band arcing which is potentially capable of spreading all over the surface and result in overall flashover.

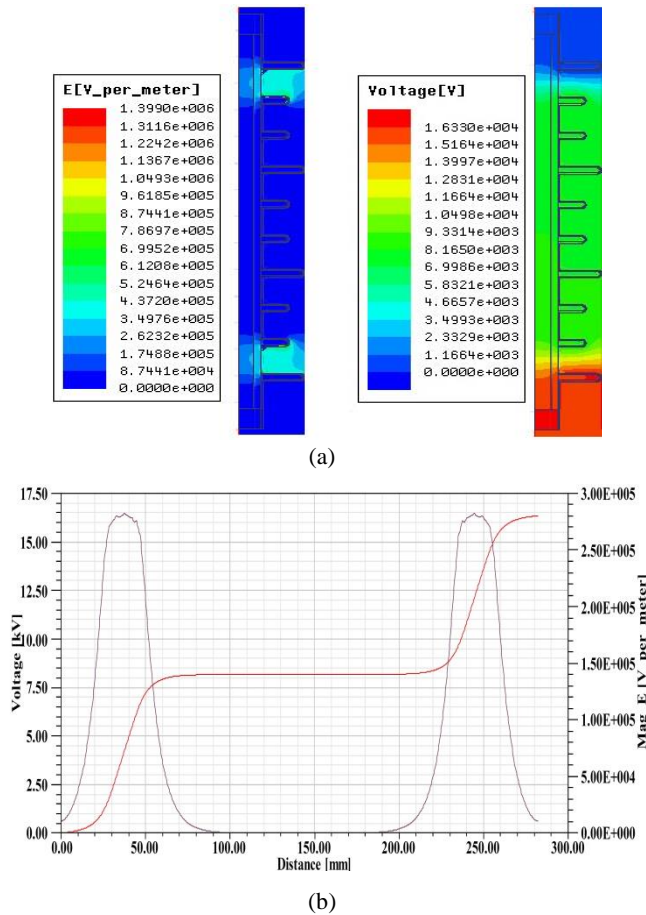


Fig. 6. The electric field and potential distributions in polluted and hydrophilic insulator with upper-lower dry bands; (a) graphical diagram of total distributions, (b) distributions in FRP core.

REFERENCES

- [1] Chaou A, Mekhaldi A, Tegar M. 2015. "Recurrence quantification analysis as a novel LC feature extraction technique for the classification of pollution severity on HV insulator model", *IEEE Transaction on Dielectric and Electrical Insulation*, 22: 3376-3384.
- [2] Ahmadi-Joneidi I, Majzoobi A, Shaygani-Akmal A, Mohseni H. 2013. "Aging evaluation of silicone rubber insulators using leakage current and flashover voltage analysis", *IEEE Transaction on Dielectric and Electrical Insulation*, 20: 212-220.
- [3] Li J, Sun C, Sebo S. 2011. "Humidity and contamination severity impact on the leakage currents of porcelain insulators", *IET Generation Transmission Distribution*. 5: 19-28.
- [4] Chandrasekar S, Kalaivanan C. 2009. "Investigations on leakage current and phase angle characteristics of porcelain and polymeric insulator under contaminated conditions", *IEEE Transaction on Dielectric and Electrical Insulation*, 16: 574-583.
- [5] Ahmadi-Joneidi I, Kamarposhti M, Shaygani-Akmal A, Mohseni H. 2013. "Leakage current analysis, FFT calculation and electric field distribution under water droplet on polluted silicon rubber insulator", *Electrical Engineering* 95: 315-323.
- [6] Jiang Y, Mcmeekin S, Reid A, Nekahi A. 2016. "Monitoring contamination level on insulator materials under dry condition with a microwave reflect meter", *IEEE Transaction on Dielectric and Electrical Insulation*, 23: 1427-1434.
- [7] Dhahbi N, Beroual A. 2015. "Time-frequency analyses of leakage current waveforms of high voltage insulators in uniform and non-uniform polluted conditions," *IET Science, Measurement and Technology*, 9: 945-954.
- [8] Natarajan A, Narayanan S. 2015. "S-transform based time-frequency analysis of leakage current signals of transmission line insulators under polluted conditions", *J Electrical Engineering Technology*, 10: 616-624.
- [9] Li J, Sima W, Sun C, Sebo S. 2010. "Use of leakage currents of insulators to determine the stage characteristics of the flashover level prediction", *IEEE Transaction on Dielectric and Electrical Insulation*, 17: 490-501.
- [10] Bashir N, Ahmad H. 2010. "Odd harmonics and third to fifth harmonic ratios of leakage currents as diagnostic tools to study the aging of glass insulators", *IEEE Transaction on Dielectric and Electrical Insulation*, 17: 819-832.
- [11] Kannan K, Shivakumar R, Chandrasekar S. 2016. "A random forest model based pollution severity classification scheme of high voltage transmission line insulators", *Journal of Electrical Engineering Technology*, 11: 951-960.
- [12] Jiang X, Shi Y, Zhang Z, Sun C. 2010. "Evaluating the safety condition of porcelain insulators by the time and frequency characteristics of LC based on artificial pollution tests", *IEEE Transaction on Dielectric and Electrical Insulation*, 17: 481-489.
- [13] Du B, Liu Y., "Frequency distribution of leakage current on silicone rubber insulator in salt-fog environments", *IEEE Transaction on Power Delivery*, 24: 1458-1464.
- [14] ManzariTavakoli M. M., Hosseini S. M. H. 2017. "The Effects of Applied Voltage, Contamination Level and the Length of Dry-Bands on the Electric Field and Leakage Current of Polymeric Insulator", *Engineering Letters*, Vol 25, Issue 3: 255-261.
- [15] Hosseini S. M. H., ManzariTavakoli M. M. 2017. "Investigation of the Influence of Hydrophobicity and Dry Band on the Electric Field and Potential Distributions in Silicon Rubber Insulator", *Conference: International Multi-Conference of Engineers and Computer Scientists 2017 Vol II, IMECS 2017, March 15 - 17, Hong Kong*.
- [16] *Hydrophobicity Classification Guide*. Swedish Transmission Research Institute (STRI), 1992; 1: 1-16.
- [17] Samimi M, Mostajabi A, Ahmadi-Joneidi I, Shaygani-Akmal A, Mohseni H. 2013. "Performance evaluation of insulators using flashover voltage and leakage current", *Electrical Power Component System*, 41: 221-233.
- [18] IEC Standard 60815, "Selection and dimensioning of high voltage insulators intended for use in polluted conditions", *IEC Standard*, Edition 1.0, 2008.
- [19] Öztürk D, Cebeci M. 2013. "Calculation of surface leakage current on high voltage insulators by ant colony algorithm-supported FEM", *Turkish Journal of Electrical Engineering*, 23: 1009-1024.